J. Phys. Chem. A **2001,** *105,* 5131−5136 **5131**

Kinetics of the Reactions of $Cl(^2P_{1/2})$ and $Cl(^2P_{3/2})$ Atoms with C_2H_6, C_2D_6, CH_3F, C_2H_5F, and CH_3CF_3 at 298 K

Kanami Hitsuda, Kenshi Takahashi, and Yutaka Matsumi*

Solar-Terrestrial Environment Laboratory and Graduate School of Science, Nagoya University, Honohara 3-13, Toyokawa, Aichi, 442-8507 Japan

Timothy J. Wallington

Ford Research Laboratory, SRL-3083, Ford Motor Company, Dearborn, Michigan 48121

Received: September 13, 2000; In Final Form: March 15, 2001

The title reactions were studied using laser flash photolysis in conjunction with laser-induced fluorescence techniques. Separate monitoring of the two spin−orbit states, $Cl(^2P_{1/2})$ and $Cl(^2P_{3/2})$, was used to measure the kinetics of the reactions of $Cl(^2P_{3/2})$ with C_2H_6, C_2D_6, CH_3F, C_2H_5F, and CH_3CF_3, the reaction of $Cl(^2P_{1/2})$ with C_2H_6, and the relaxation of $Cl(^2P_{1/2})$ by collisions with C_2H_6, C_2D_6, CH_3F, C_2H_5F, and CH_3CF_3. Measured reaction rate constants were (units of cm^3 $molecule^{-1}$ s^{-1}): $k(Cl(^2P_{3/2}) + C_2H_6) = (5.85 \pm 0.55) \times 10^{-11}$, $k(Cl(^2P_{3/2}) + C_2D_6) = (1.87 \pm 0.12) \times 10^{-11}$, $k(Cl(^2P_{3/2})+ CH_3F) = (2.7 \pm 0.2) \times 10^{-13}$, $k(Cl(^2P_{3/2}) + CH_3CH_2F) = (6.8 \pm 0.5) \times 10^{-12}$, and $k(Cl(^2P_{3/2}) + CH_3CF_3) < 1 \times 10^{-14}$ cm^3 $molecule^{-1}$ s^{-1}. Measured relaxation rate constants for deactivation of $Cl(^2P_{1/2})$ to $Cl(^2P_{3/2})$ via collisions with C_2H_6, C_2D_6, CH_3F, C_2H_5F, CH_3CF_3, and CF_4 were $(1.22 \pm 0.09) \times 10^{-10}$, $(2.4 \pm 0.2) \times 10^{-10}$, $(6.4 \pm 0.5) \times 10^{-11}$, $(1.9 \pm 0.2) \times 10^{-10}$, $(2.0 \pm 0.2) \times 10^{-10}$, and $(2.3 \pm 0.4) \times 10^{-11}$, respectively. Collisions of $Cl(^2P_{1/2})$ with C_2H_6 and C_2D_6 resulted mainly in the relaxation of $Cl(^2P_{1/2})$ to $Cl(^2P_{3/2})$ and not in the reactive formation of HCl (DCl). The rate constant of the reactive path for $Cl(^2P_{1/2}) + C_2H_6$ was $< 3 \times 10^{-11}$ cm^3 $molecule^{-1}$ s^{-1}.

Introduction

Chlorine atoms play an important role in stratospheric chemistry[1,2] and are used widely in the laboratory to mimic OH radicals in studies of the oxidation mechanisms of organic compounds.[3−5] The spin−orbit $Cl(^2P_{1/2})$ and $Cl(^2P_{3/2})$ states are separated by 2.52 kcal/mol (882 cm^{-1}) and at ambient temperature there is an appreciable population of the excited $Cl(^2P_{1/2})$ state (0.71% at 298 K). Many different kinetic techniques have been applied to study the reactions of Cl atoms with organic compounds, and there is now a large kinetic database concerning such reactions at ambient temperature.[6] The existing kinetic database for $Cl(^2P)$ does not differentiate between the reactivity of the $Cl(^2P_{3/2})$ and $Cl(^2P_{1/2})$ states. The reactivities of these two spin−orbit states are expected to be considerably different. In reactions of halogen atoms, the ground spin−orbit state $^2P_{3/2}$ is generally considered to be more reactive than the $^2P_{1/2}$ state due to the adiabatic nature of the corresponding potential surfaces.[7] However, there is little information concerning the relative importance of the $Cl(^2P_{1/2})$ and $Cl(^2P_{3/2})$ states in the reactions of Cl atoms with organic compounds.[8] This raises the question: "To what extent does the small (0.71% at 298 K) population of $Cl(^2P_{1/2})$ contribute to the observed overall reactivity of Cl atoms toward organic compounds?" To answer this question laser flash photolysis−laser-induced fluorescence techniques have been applied to study the reactivity of both $Cl(^2P_{1/2})$ and $Cl(^2P_{3/2})$ with C_2H_6, C_2D_6, CH_3F, C_2H_5F, and CH_3CF_3. We find that collisional deactivation of spin−orbit excited $Cl(^2P_{1/2})$ atoms occurs at rates close to the gas kinetic limit and that $Cl(^2P_{1/2})$ atoms are substantially (at least a factor of 2) less reactive than $Cl(^2P_{3/2})$ atoms. Under ambient conditions $Cl(^2P_{1/2})$ atoms are responsible for <0.4% and <1.4% of the observed reactivity of thermalized Cl atoms toward C_2H_6 and C_2D_6.

Experimental Section

Experiments were conducted using the laser flash photolysis laser-induced fluorescence (LIF) apparatus, which is shown schematically in Figure 1. The experimental setup is the almost same as that in ref 8. The reactant gases were flowed into the reaction cell which was continuously evacuated by a rotary pump. $Cl(^2P_j)$ atoms were produced by the 193 nm photolysis of HCl which produces 59% $Cl(^2P_{3/2})$ and 41% $Cl(^2P_{1/2})$.[9]

$$\begin{aligned} HCl + h\nu\ (193\ nm) &\rightarrow H + Cl(^2P_{3/2}) \\ &\rightarrow H + Cl(^2P_{1/2}) \end{aligned}$$

From a consideration of the absorption coefficient of HCl at 193 nm and the power density of the photolysis laser, we estimate the initial Cl atom concentration in the present experiments to be in the range $(1-5) \times 10^{12}$ cm^{-3}. The Cl atoms produced from the photodissociation of HCl have relatively little translational excitation, since most of the excess energy goes into the translational energy of the H atoms to conserve momentum in the system. Nevertheless, buffer gases were added to the reactant mixtures to suppress hot atom effects in the kinetic study. $Cl(^2P_{1/2})$ and $Cl(^2P_{3/2})$ were monitored using VUV-LIF at 134.724 nm (4s $^2P_{3/2} \rightarrow$ 3p $^2P_{3/2}$) and 135.166 nm (4s $^2P_{1/2} \rightarrow$ 3p $^2P_{1/2}$). The tunable probe vacuum UV light was

---

* Corresponding author. E-mail: matsumi@stelab.nagoya-u.ac.jp.

10.1021/jp003222s CCC: $20.00

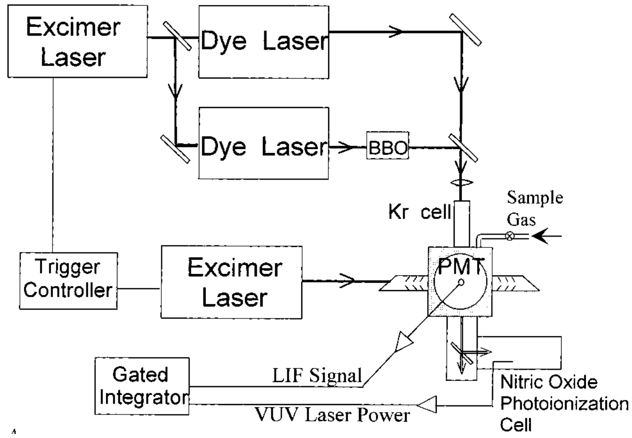

Figure 1. Schematic diagram of apparatus.

generated by four-wave mixing ($2\omega_1 - \omega_2$) in Kr gas using two dye lasers pumped by a single XeCl excimer laser (λ = 308 nm).[10] The wavelength of ω_1 was 212.56 nm corresponding to a two-photon resonance to the Kr $5p[1/2]_0$ state. The wavelength of ω_2 was tuned near 500 nm. Typical pulse energies were 0.2 and 4 mJ for 212.56 and 500 nm light, respectively. The ω_1 and ω_2 light beams were focused into a cell containing Kr gas at 15−20 Torr. The resulting vacuum UV light beam passed through a LiF window into the reaction cell.

The VUV-LIF signal from $Cl(^2P_{1/2})$ or $Cl(^2P_{3/2})$ was detected by a solar blind photomultiplier tube mounted at right angles to the propagation direction of the probing VUV beam and the 193 nm photolysis beam. The 193 nm laser light and the vacuum UV laser light perpendicularly crossed in the reaction cell. The time delay between the dissociation and probe laser pulses was controlled by a pulse generator (Stanford Research, DG535), and the jitter of the delay time was less than 10 ns. Both pump and probe lasers were operated with the repetition rate of 10 Hz. In typical experiments, the delay time was scanned to cover the whole time domain of the fluorescence signal decay, usually $t = 0-300\ \mu s$ (with step $\Delta t = 1.5\ \mu s$) for the Cl*. At each step, the signal was averaged for 10 laser shots, and total time of the decay profile measurement was 200s.

Chlorine atoms have nuclear spin I = 3/2 for both ^{35}Cl and ^{37}Cl, which causes hyperfine couplings, $\mathbf{F} = \mathbf{I} + \mathbf{J}$. Since the value of the quadruple coupling constant *eq*Q for the free chlorine atom ^{35}Cl is 110 MHz,[11] the energy splitting among the hyperfine structure is much smaller than the laser line width (> 10 GHz). Although relaxation of the hyperfine structure levels is slow in the $^2P_{1/2}$ state[16] and fast in the $^2P_{3/2}$ state, the distributions among the hyperfine levels do not concerned our Cl reaction experiments.

Two sets of experiments were performed. First, the reactivity of ground spin−orbit state $Cl(^2P_{3/2})$ atoms toward C_2H_6, C_2D_6, CH_3F, C_2H_5F, and CH_3CF_3 was measured by photolysis of HCl/reactant mixtures in 0.2−1.2 Torr of CF_4 diluent. Pressure of the reactants in the reaction cell was monitored by a capacitance manometer. CF_4 is an efficient relaxation agent for $Cl(^2P_{1/2})$ atoms with a collision quenching rate constant of 2.4×10^{-11} cm^3 molecule^{-1} s^{-1}.[12] In the presence of 0.2−1.2 Torr of CF_4, the $Cl(^2P_{1/2})$ atoms have a lifetime which is less than 8 μs with respect to relaxation to the ground spin−orbit state. After relaxation of >90% of the $Cl(^2P_{1/2})$ atoms the subsequent decay of $Cl(^2P_{3/2})$ atoms was monitored and used to derive kinetic data for reactions of $Cl(^2P_{3/2})$ atoms with C_2H_6, C_2D_6, CH_3F, C_2H_5F, and CH_3CF_3. Second, the temporal profiles of $Cl(^2P_{1/2})$ and $Cl(^2P_{3/2})$ atoms were monitored following the photolysis of HCl/reactant mixtures in 0.2−1.5 Torr of Ar diluent. Ar is an inefficient relaxation agent for $Cl(^2P_{1/2})$ atoms (quenching rate constant = $(3 \pm 1) \times 10^{-16}$ cm^3 molecule^{-1} s^{-1} [13]). By monitoring temporal profiles of $Cl(^2P_{1/2})$ and $Cl(^2P_{3/2})$ atoms kinetic data was derived for the reactivity of $Cl(^2P_{1/2})$ toward the reactants. In all experiments the concentration of added reactants was at least 100 times greater than the initial Cl atom concentration. Accordingly, the loss of Cl atoms is expected to follow pseudo first-order kinetics.

Reaction mixtures were prepared in storage bulbs by mixing the precursor (HCl) with reactant (C_2H_6, C_2D_6, CH_3F, C_2H_5F, or CH_3CF_3) and buffer gas (CF_4 or Ar). The gases used in the experiments had the following stated purities: HCl, 99.9%; C_2H_6, 99.99%; C_2D_6, 99.9%; CH_3F, 99%; C_2H_5F, 99.9%; CH_3CF_3, 99.9%; CF_4, 99.99%; and Ar, 99.999%. All gases were used without further purification.

Results

1. Loss of $Cl(^2P_{1/2})$ Atoms in Collisions with HCl and CF_4. Prior to studying the reactivity of $Cl(^2P_{3/2})$ and $Cl(^2P_{1/2})$, experiments were performed to investigate the loss of $Cl(^2P_{1/2})$ atoms in collisions with HCl. Loss of $Cl(^2P_{1/2})$ atoms following flash photolysis of HCl/Ar mixtures was monitored using VUV-LIF at 134.724 nm. In all cases the loss of $Cl(^2P_{1/2})$ atoms followed first-order kinetics with pseudo first-order constants which increased linearly with the HCl concentration. The loss of $Cl(^2P_{1/2})$ atoms reflects both quenching by, and reaction with, HCl (we make the reasonable assumption that chemical reaction of $Cl(^2P_{1/2})$ atoms with HCl produces ground-state $Cl(^2P_{3/2})$ atoms). The overall removal rate constant (quenching plus reaction) for interaction of $Cl(^2P_{1/2})$ atoms with HCl was measured in the present work to be $(7.8 \pm 0.8) \times 10^{-12}$ cm^3 molecule^{-1} s^{-1}. This result is somewhat lower than the values of $(1.2 \pm 0.2) \times 10^{-11}$ reported by Tiemann et al.[14] and $(1.2 \pm 0.3) \times 10^{-11}$ cm^3 molecule^{-1} s^{-1} by Chichinin,[15] and a little larger than the value of 6×10^{-12} by Donovan et al.[16] The causes of these small disagreements are unclear. In the experiments described in the following sections the HCl concentration was $(1-5) \times 10^{14}$ cm^{-3}. Under these experimental conditions the pseudo first-order rate of removal of $Cl(^2P_{1/2})$ atoms via quenching/reaction with HCl was 800−4000 s^{-1} and was of negligible importance compared to loss of $Cl(^2P_{1/2})$ atoms via collisions with the reactants described below.

To investigate the rate of relaxation of $Cl(^2P_{1/2})$ to $Cl(^2P_{3/2})$ via collisions with CF_4 the temporal profile of $Cl(^2P_{1/2})$ atoms was monitored following flash photolysis of HCl/CF_4 mixtures. The decay of $Cl(^2P_{1/2})$ atoms in such experiments followed first-order kinetics with pseudo first-order rates which increased linearly with CF_4 pressure. A rate constant of $(2.3 \pm 0.4) \times 10^{-11}$ was derived for the relaxation of $Cl(^2P_{1/2})$ by CF_4 which is consistent with the value of $(2.4 \pm 0.7) \times 10^{-11}$ cm^3 molecule^{-1} s^{-1} reported by Chichinin.[12]

2. Kinetics of the Reactions of $Cl(^2P_{3/2})$ Atoms with C_2H_6, C_2D_6, CH_3F, C_2H_5F, and CH_3CF_3. Figure 2 shows the observed temporal profiles of the two spin−orbit states following the 193 nm pulsed irradiation of a mixture of 3 mTorr of HCl and 0.11 Torr of C_2H_6 in 0.60 Torr of CF_4 diluent. The *y*-axis scale in Figure 2 is the observed fluorescence intensity at 134.724 and 135.166 nm from $Cl(^2P_{1/2})$ and $Cl(^2P_{3/2})$, respectively, in arbitrary units. We are not able to provide an absolute calibration of the $Cl(^2P_{1/2})$ and $Cl(^2P_{3/2})$ concentrations. The relative strengths of the initial fluorescence signals at 134.724 and 135.166 nm given in Figure 2 have been scaled to reproduce the expected 41:59 ratio of $Cl(^2P_{1/2})$ and $Cl(^2P_{3/2})$ formation from the photolysis of HCl.[9]

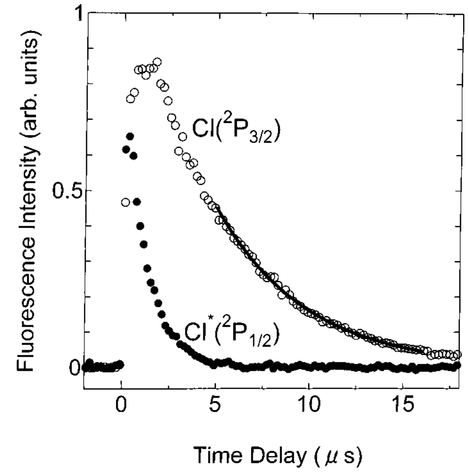

Figure 2. Observed decay of Cl($^2P_{1/2}$) (filled circles) and Cl($^2P_{3/2}$) (open circles) following flash photolysis of a mixture containing 3 mTorr of HCl and 0.11 Torr of C_2H_6 in 0.60 Torr of CF_4 diluent at 298 K. The solid line is a first-order decay fit to the Cl($^2P_{3/2}$) data at a time (>5 μs) when >90% of Cl($^2P_{1/2}$) had decayed.

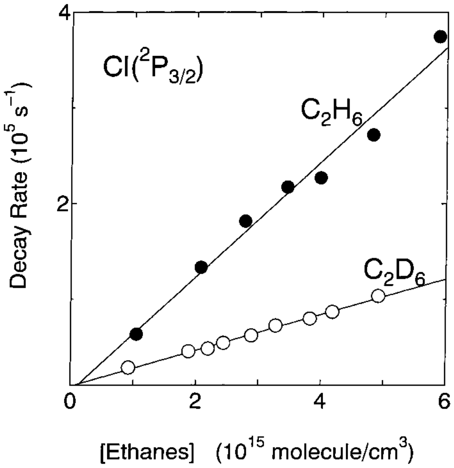

Figure 3. Plot of pseudo first-order loss of Cl($^2P_{3/2}$) atoms versus the partial pressure of ethane (filled symbols = C_2H_6, open symbols = C_2D_6).

The time-resolved VUV-LIF signal of Cl($^2P_{1/2}$) and Cl($^2P_{3/2}$) atoms produced by the photolysis of HCl exhibits a fast rise ($t < 0.2$ μs) followed by a slower decay. The presence of CF_4 diluent rapidly relaxes the excited spin−orbit state. The subsequent decay of Cl($^2P_{3/2}$) atoms follows pseudo first-order kinetics and provides information on the kinetics of the Cl + C_2H_6 reaction.

Figure 3 shows a plot of the observed pseudo first-order decay of Cl($^2P_{3/2}$) atoms in the presence of C_2H_6 and C_2D_6 reactants. The lines in Figure 3 are linear least-squares fits. The slopes of the least-squares fits give the rate constants k(Cl($^2P_{3/2}$) + C_2H_6) = (5.85 ± 0.55) × 10^{-11} and k(Cl($^2P_{3/2}$) + C_2D_6) = (1.87 ± 0.12) × 10^{-11} cm^3 molecule^{-1} s^{-1}. Quoted uncertainties are two standard deviations from the least-squares fits and also some systematic errors such as the precision of the concentrations are considered. Similar experiments were performed using CH_3F, C_2H_5F, and CH_3CF_3 reactants. The measured rate constants are presented in Table 1.

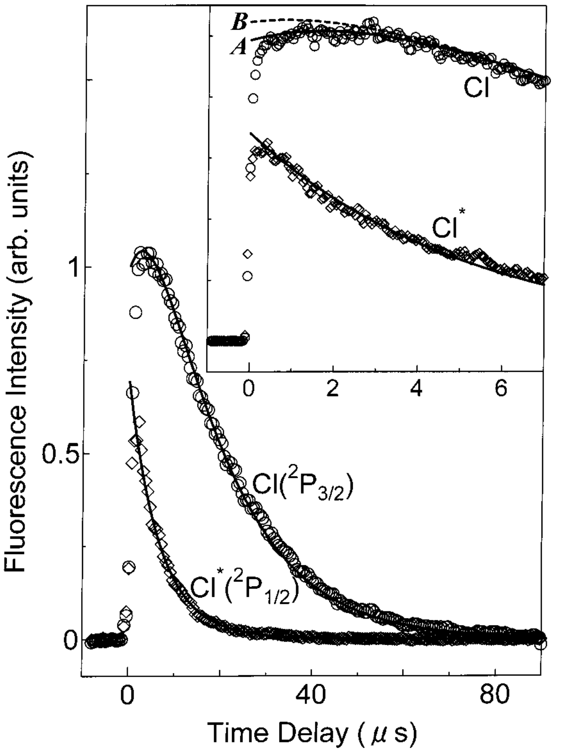

Figure 4. Observed decay of Cl($^2P_{1/2}$) (diamonds) and Cl($^2P_{3/2}$) (circles) following flash photolysis of a mixture containing 3 mTorr of HCl and 35 mTorr of C_2H_6 in 0.23 Torr of Ar diluent at 298 K. The insert shows the data for the first 8 μs following the photolysis flash. The thick solid curve "A" is the fit to the Cl($^2P_{3/2}$) data assuming k_3/k_1 = 0.0 while the short dash curve B is the result assuming k_3/k_1 = 0.5, see text for details. Each time profiles are averaged over 4−10 times running.

TABLE 1: Kinetic Data for Reactions of Cl($^2P_{3/2}$) Atoms (measured in this work) and Thermalized Cl Atoms (reported previously) with Several Organic Compounds at 298 ± 2 K

reactant	k(Cl($^2P_{3/2}$) + reactant) cm^3 molecule^{-1} s^{-1}	reference
C_2H_6	(5.75 ± 0.45) × 10^{-11}	Tyndall et al.[21]
	(5.7 ± 0.6) × 10^{-11}	NASA JPL Panel[22]
	(5.9 ± 0.8) × 10^{-11}	IUPAC Panel [23]
	(5.85 ± 0.55) × 10^{-11}	this work
C_2D_6	(1.9± 0.5) × 10^{-11}	Tschuikow-Roux et al.[29]
	(0.83 ± 0.07) × 10^{-11}	Parmar and Benson [26]
	(1.85 ± 0.13) × 10^{-11}	Wallington and Hurley[30]
	(2.11 ± 0.05) × 10^{-11}	Dobis et al.[27]
	(1.87 ± 0.12) × 10^{-11}	this work
CH_3F	(3.61 ± 0.10) × 10^{-13}	Manning and Kurylo[28]
	(4.21 ± 1.27) × 10^{-13}	Tschuikow-Roux et al.[31]
	(3.40 ± 0.70) × 10^{-13}	Tuazon and Atkinson[32]
	(3.24 ± 0.54) × 10^{-13}	Wallington et al.[33]
	(2.7 ± 0.2) × 10^{-13}	this work
CH_3CH_2F	(6.90 ± 2.14) × 10^{-12}	Tschuikow-Roux et al.[31]
	(6.8 ± 0.5) × 10^{-12}	this work
CF_3CH_3	(2.49 ± 0.83) × 10^{-17}	Tschuikow-Roux et al.[31]
	<1 × 10^{-14}	this work

3. Kinetics of the Reactions of Cl($^2P_{1/2}$) Atoms with C_2H_6 and C_2D_6. To investigate the reactivity of Cl($^2P_{1/2}$) atoms with C_2H_6 and C_2D_6, experiments were performed using Ar as the diluent gas. Argon is an inefficient quencher of Cl($^2P_{1/2}$) atoms (quenching rate constant = 3.0 × 10^{-16} cm^3 molecule^{-1} s^{-1} [13,17−18]) and its use as diluent facilitates investigation of the reactivity of spin−orbit excited Cl atoms. Figure 4 shows thetemporal profiles of the two spin−orbit states following laser flash photolysis of a mixture of 3 mTorr of HCl and 35 mTorr of C_2H_6 in 0.23 Torr total pressure using Ar diluent. The insert in Figure 4 shows the first 8 μs in more detail.

The shape of the profiles of Cl($^2P_{3/2}$) and Cl($^2P_{1/2}$) atoms in Figure 4 provides insight into the reactivity of Cl($^2P_{1/2}$) with

C_2H_6. The reactions occurring in the system are the following:

$$Cl(^2P_{3/2}) + C_2H_6 \rightarrow HCl + C_2H_5 \quad \text{Chemical reaction} \qquad (1)$$

$$Cl(^2P_{3/2}) + C_2H_6 \rightarrow Cl(^2P_{1/2}) + C_2H_6 \quad \text{Excitation} \qquad (2)$$

$$Cl(^2P_{1/2}) + C_2H_6 \rightarrow HCl + C_2H_5 \quad \text{Chemical reaction} \qquad (3)$$

$$Cl(^2P_{1/2}) + C_2H_6 \rightarrow Cl(^2P_{3/2}) + C_2H_6 \quad \text{Relaxation} \qquad (4)$$

As discussed above, at 298 K only 0.71% of thermalized Cl atoms reside in the $Cl(^2P_{1/2})$ state. Hence, for the conditions shown in Figure 4, loss of $Cl(^2P_{1/2})$ via relaxation to $Cl(^2P_{3/2})$ far exceeds the rate of excitation of $Cl(^2P_{3/2})$ to $Cl(^2P_{1/2})$. To a first approximation, reaction 2 can be neglected during the first 10 μs and the $Cl(^2P_{1/2})$ profile is determined by loss via reactions 3 and 4. Accordingly, as seen in Figure 4 the loss of $Cl(^2P_{1/2})$ follows a simple exponential form with a pseudo first-order rate constant $= (k_3 + k_4)[C_2H_6]$.

The $Cl(^2P_{3/2})$ profile is expected to follow either an exponential or a nonexponential profile depending on the relative magnitudes of reactions 3 and 4. If reaction 3 is much more important than reaction 4 as a loss mechanism for $Cl(^2P_{1/2})$ then the profiles of $Cl(^2P_{3/2})$ and $Cl(^2P_{1/2})$ will be essentially decoupled and both will follow simple exponential kinetics. If, on the other hand, reaction 4 is much more important than reaction 3 then there will be significant repopulation of $Cl(^2P_{3/2})$ via relaxation of $Cl(^2P_{1/2})$ leading to a delay in the observed $Cl(^2P_{3/2})$ decay and nonexponential kinetics. As seen from Figure 4, there is indeed a delay in the observed decay of the $Cl(^2P_{3/2})$ signal which shows that reaction 4 is more important than reaction 3 as a loss mechanism for $Cl(^2P_{1/2})$ atoms.

To provide quantification of the relative importance of reactions 1−4, expressions 5 and 6 were evaluated and compared to the observed $Cl(^2P_{3/2})$ and $Cl(^2P_{1/2})$ profiles, $Cl^* = Cl(^2P_{1/2})$.

$$\frac{d[Cl^*]}{dt} = -(k_3 + k_4)[Cl^*][C_2H_6] + k_2[Cl][C_2H_6] \qquad (5)$$

$$\frac{d[Cl]}{dt} = -(k_1 + k_2)[Cl][C_2H_6] + k_4[Cl^*][C_2H_6] \qquad (6)$$

Values for $(k_3 + k_4)[C_2H_6]$ were obtained from the exponential decay of the $Cl(^2P_{1/2})$ signal, the value of $k_1 = (5.85 \pm 0.55) \times 10^{-11}$ cm^3 molecule^{-1} s^{-1} was taken from the previous section. The analytical solution for a system of two differential equations was reported by Chasovnikov et al.[19] In the present study, the simultaneous differential equations, eqs 5 and 6, were numerically solved to obtain the temporal behavior of $Cl(^2P_{3/2})$ using a Runge−Kutta method. The detailed balance principle was assumed between the excitation and relaxation rate constants, k_2 and k_4. The solid lines through the $Cl(^2P_{3/2})$ data in the insert in Figure 4 show the predicted behavior with $k_3/k_1 = 0.5$ (indicated by "A" in Figure 4) and 0 (B). It is clear that there is little, or no, experimental evidence for a reaction of $Cl(^2P_{1/2})$ with C_2H_6. From a visual inspection of the data trend we derive $k_3/k_1 < 0.5$. In similar fashion we were able to derive an upper limit of $k_3/k_4 < 0.3$. Experiments were also performed using C_2D_6 as reactant, the results are given in Table 2.

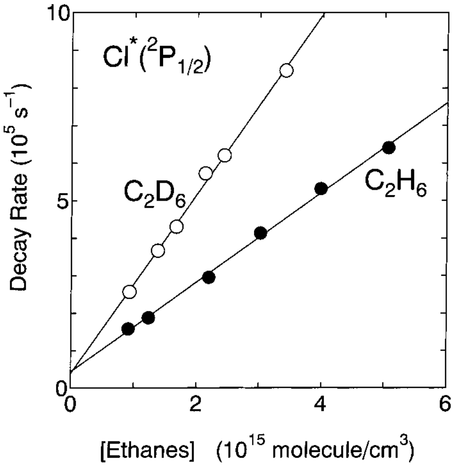

Figure 5. Plot of pseudo first-order loss of $Cl(^2P_{1/2})$ atoms versus the partial pressure of ethane (filled symbols = C_2H_6, open symbols = C_2D_6). The loss of $Cl(^2P_{1/2})$ atoms is attributed primarily to collisional quenching, see text for details.

TABLE 2: Relative Importance of Processes (1), (3), and (4) for $Cl(^2P_{1/2})$ Atoms

reactant	k_3/k_1	k_3/k_4
C_2H_6	<0.5	<0.3
C_2D_6	<2.0	0.3

4. Quenching of $Cl(^2P_{1/2})$ Atoms in Collisions with C_2H_6, C_2D_6, CH_3F, C_2H_5F, and CH_3CF_3. The rate of decay of the VUV-LIF attributable to $Cl(^2P_{1/2})$ following the laser flash photolysis of HCl/reactant/Ar mixtures provides information on the rate of collisional quenching of $Cl(^2P_{1/2})$ atoms. In all experiments the decay of $Cl(^2P_{1/2})$ atoms followed first-order kinetics. Figure 5 show plots of the observed pseudo first-order loss rates of $Cl(^2P_{1/2})$ versus the concentration of ethane in experiments using either C_2H_6 or C_2D_6. As discussed in the previous section, the experiments suggest that chemical reaction of $Cl(^2P_{1/2})$ atoms with C_2H_6 is unimportant and we attribute the $Cl(^2P_{1/2})$ decay to quenching physical quenching by collision with C_2H_6. As seen from Figure 5, the rate of $Cl(^2P_{1/2})$ decay increased linearly with $[C_2H_6]$. Linear least-squares analysis of the data in Figure 5 gives quenching rate constants of $(1.22 \pm 0.09) \times 10^{-10}$ and $(2.4 \pm 0.02) \times 10^{-10}$ cm^3 molecule^{-1} s^{-1} for C_2H_6 and C_2D_6, respectively. The fact that C_2D_6 is twice as efficient as C_2H_6 in relaxing $Cl(^2P_{1/2})$ presumably reflects a better match between the energy levels in C_2D_6 and the $Cl(^2P_{1/2})$ to $Cl(^2P_{3/2})$ transition. Measured quenching efficiencies of CH_3F, C_2H_5F, and CH_3CF_3 are given in Table 3.

Discussion

1. Kinetics of the Reactions of $Cl(^2P_{1/2})$ Atoms with C_2H_6 and C_2D_6. While there has been considerable study of spin−orbit effects in gas-phase reactions[7] there is little data available concerning such effects in reactions of Cl atoms with organic compounds. It has been shown that the relaxation of $Cl(^2P_{1/2})$ to $Cl(^2P_{3/2})$ is the dominant process occurring in collisions of $Cl(^2P_{1/2})$ with CH_4.[8,13] Recently, Lee and Liu[20] studied the Cl + H_2 reaction system using a crossed beam apparatus. They indicated that the excited-state $Cl(^2P_{1/2})$ is more reactive to H_2 than the $Cl(^2P_{3/2})$ state by at least a factor of 6 at the collision energy of 5.2 kcal mol^{-1} used in the crossed beam. The symmetry consideration for the Cl + H_2 reaction system indicates that the $Cl(^2P_{3/2}) + H_2$ reactant state correlates to the $HCl(X^1\Sigma) + H$ product state adiabatically while the $Cl(^2P_{1/2}) + H_2$ state does not correlate to the $HCl(X^1\Sigma) + H$ state ($Cl(^2P_{1/2}) + H_2$ correlates to the high-lying electronic state $HCl^* + H$). Therefore, the reaction from $Cl(^2P_{1/2}) + H_2$ to $HCl(X^1\Sigma) + H$ is adiabatically forbidden. The high reactivity of $Cl(^2P_{1/2})$ observed by Lee and Liu[20] in the Cl + H_2 system is attributed

TABLE 3: Total Deactivation Rate Constants of $Cl^*(^2P_{1/2})$ in Collisions with Several Molecules and the Vibrational Frequencies of the Collision Partners

collison partner	relaxation rate constant (cm^3 molecule^{-1} s^{-1})	ref	IR active mode frequency, ν (cm^{-1})[a]	$\Delta\nu = \nu - 882$ (cm^{-1})	IR band intensity[a]
C_2H_6	$(1.22 \pm 0.09) \times 10^{-10}$	*b*	ν_{12} 822	−60	s
C_2D_6	$(2.4 \pm 0.2) \times 10^{-10}$	*b*	ν_6 1077	195	
			ν_{11} 1081	199	
			ν_{12} 594	−288	
CH_3F	$(0.64 \pm 0.05) \times 10^{-10}$	*b*	ν_3 1049	167	
			ν_6 1182	300	
CH_3CH_2F	$(1.9 \pm 0.2) \times 10^{-10}$	*b*	ν_8 1108	226	vs
			ν_9 1048	166	vs
			ν_{10} 880	−2	vs
CH_3CF_3	$(2.0 \pm 0.2) \times 10^{-10}$	*b*			
HCl	$(7.8 \pm 0.8) \times 10^{-12}$	*b*			
	$(1.2 \pm 0.2) \times 10^{-11}$	*c*			
	$(1.2 \pm 0.3) \times 10^{-11}$	*d*			
	6×10^{-12}	*e*			
CF_4	$(2.3 \pm 0.4) \times 10^{-11}$	*b*			
	$(2.4 \pm 0.7) \times 10^{-11}$	*f*			

[a] Taken from NIST Chemistry WebBook (http://webbook.nist.gov/). [b] This work. [c] Ref 14. [d] Ref 15. [e] Ref 16. [f] Ref 12.

to the importance of the nonadiabatic reaction pathway at the high collision energies used (5.2 kcal mol^{-1}).

In the Cl + C_2H_6 reaction system, the activation energy barrier for formation of HCl + C_2H_5 is 0.18 kcal mol^{-1} (63 cm^{-1}), this barrier is much smaller than the spin−orbit excitation of $Cl(^2P_{1/2})$ atoms (882 cm^{-1}). If spin−orbit excitation were effective in overcoming the barrier to H-atom abstraction from C_2H_6 we would expect much greater reactivity of $Cl(^2P_{1/2})$ than $Cl(^2P_{3/2})$. However, the experimental results reported here show that spin−orbit excited Cl atoms are much less reactive (by at least a factor of 2) than ground-state Cl atoms. This result suggests that the adiabatically forbidden character between the $Cl(^2P_{1/2})$ + C_2H_6 and $HCl(X^1\Sigma)$ + C_2H_5 is still effective, although the reaction system has lower symmetry than the Cl + H_2 system. The nonadiabatic pathway of $Cl(^2P_{1/2})$ + C_2H_6 should be small under our experimental conditions due to the small collision energy of 0.6 kcal mol^{-1}.

For the reaction system of $Cl(^2P_{1/2})$ + C_2D_6, the collisional relaxation rate of $Cl(^2P_{1/2})$ to $Cl(^2P_{3/2})$ is about twice as large as that for $Cl(^2P_{1/2})$ + C_2H_6. Therefore, the estimated upper limit of the obtained ratio of the chemical reaction rate of $Cl(^2P_{1/2})$ to that of $Cl(^2P_{3/2})$, k_3/k_1, is larger for $Cl(^2P_{1/2})$ + C_2D_6 than $Cl(^2P_{1/2})$ + C_2H_6 due to the experimental restriction.

The upper limits for the reactivity spin−orbit excited $Cl(^2P_{1/2})$ atoms with C_2H_6 and C_2D_6 combined with the population of the excited state (0.71% at 298 K) lead to the conclusion that $Cl(^2P_{1/2})$ are responsible for < 0.4% and < 1.4% of the observed reactivity of thermalized Cl atoms toward C_2H_6 and C_2D_6.

2. Kinetics of the Reactions of $Cl(^2P_{3/2})$ Atoms with C_2H_6, C_2D_6, CH_3F, C_2H_5F, and CH_3CF_3. As discussed in the preceding section, the results from the present work show that $Cl(^2P_{1/2})$ atoms are responsible for <0.4% of the reactivity of thermalized Cl atoms toward C_2H_6. Hence, the reactivity of thermalized Cl atoms toward C_2H_6 measured in conventional kinetic experiments can be equated to the reactivity of the ground-state $Cl(^2P_{3/2})$. On this basis we are able to compare the kinetic data for the $Cl(^2P_{3/2})$ + C_2H_6 reaction measured here with the literature data for the reaction of thermalized Cl atoms with C_2H_6, see Table 1.

The reaction of Cl atoms with ethane has been the subject of numerous kinetic studies as reviewed recently by Tyndall et al.[21] and the NASA[22] and IUPAC[23] data evaluation panels. The dynamics of the reaction with ethane have also been studied extensively.[24,25] The kinetics of the reaction of Cl atoms with ethane are well established (perhaps the best characterized Cl atom reaction). The excellent agreement between the results from the present study and the recommendations of recent reviews (see Table 1) serves as a validation of the current experimental methodology.

Interestingly, with the exception of the early VLPR (very low-pressure reactor) study by Parmar and Benson[26] which is superseded by a more recent and more complete VLPR study by Dobis et al.,[27] there is also excellent agreement in the results of all kinetic studies of the reaction of Cl atoms with perdeuterioethane. While the reactivity of $Cl(^2P_{3/2})$ atoms toward CH_3F measured herein is approximately 20% lower than those for $Cl(^2P)$ measured in previous studies, our rate constant measured is consistent within the combined experimental uncertainties with all previous investigations except that by Manning and Kurylo.[28] The kinetic data measured here for C_2H_5F and CF_3CH_3 are consistent with the previous studies. It appears that spin−orbit excited $Cl(^2P_{1/2})$ atoms do not make a noticeable contribution to the reactivity of thermalized Cl atoms toward CH_3F and CH_3CH_2F.

3. Quenching of $Cl(^2P_{1/2})$ Atoms in Collisions with C_2H_6, C_2D_6, CH_3F, C_2H_5F, and CH_3CF_3. We have obtained the total deactivation rate constants of $Cl(^2P_{1/2})$ with C_2H_6, C_2D_6, CH_3F, C_2H_5F, and CH_3CF_3, which are listed in Table 3. The quenching rate constants for C_2H_6, C_2D_6, CH_3F, C_2H_5F, and CH_3CF_3 are close to the gas-kinetic collision rate (order of 10^{-10} cm^3 molecule^{-1} s^{-1}). Chichinin[12] measured quenching rate constants of $Cl(^2P_{1/2})$ with various molecules using time-resolved laser magnetic resonance (LMR) and also summarized the experimental data of the quenching rate constants of $Cl(^2P_{1/2})$ with more than 30 molecules. The quenchers agents C_2H_6, C_2D_6, CH_3F, C_2H_5F, and CH_3CF_3 which were used in the present study (Table 3) are not listed in his summary table. Chichinin suggested that E−V energy exchange is the dominant route for $Cl(^2P_{1/2})$ quenching in most cases, and proposed the following expression for deactivation of $Cl(^2P_{1/2})$ by quencher M:

$$k_{qM} = \sum_i A\left(\frac{I_i}{\nu_i}\right)\exp\left(-\frac{|\Delta E_i|}{B}\right) \qquad (7)$$

where k_{qM} is the quenching rate constant of $Cl(^2P_{1/2})$ by the quencher M, summation is over vibrational modes of the quencher, I_i and ν_i are the intensity in units of cm^2 molecule^{-1} s^{-1} and frequency of the ith absorption band of the quencher, $\Delta E_i \equiv h\nu_i - 882$ cm^{-1} is the energy defect of the $E-V$ transfer process, and *A* and *B* are parameters. From fitting expression 7 to the experimentally measured quenching rate constants Chichinin[12] reported values of 145 and 77 cm^{-1} for A and B, respectively.

Table 3 lists the IR active vibrational frequencies (and band intensities) near to the spin−orbit energy difference between Cl($^2P_{1/2}$) and Cl($^2P_{3/2}$) (882 cm^{-1}) of the gases studied in the present work. The frequencies and the band intensities are taken from NIST Chemistry WebBook (http://webbook.nist.gov/) where available. As listed in Table 3, C_2H_6 has a vibrational frequency mode which is much closer to the Cl atom spin−orbit energy difference than does C_2D_6. It seems reasonable to assume that IR band intensities of C_2H_6 and C_2D_6 are not substantially different. Counter to the experimental observations, expression 7 predicts that C_2H_6 is a much more efficient quenching agent than C_2D_6. The experimental results of the present work cast doubt on the utility of expression 7 to predict the quenching rates for Cl($^2P_{1/2}$).

Conclusions

We have studied the reaction kinetics of Cl with C_2H_6, C_2D_6, CH_3F, C_2H_5F, and CH_3CF_3. The vacuum ultraviolet laser-induced fluorescence technique combined with the laser flash photolysis technique made it possible to detect the temporal behaviors of the spin−orbit components of Cl atom, Cl($^2P_{1/2}$) and Cl($^2P_{3/2}$), independently. The kinetic data measured here for the Cl atom reactions are consistent with the previous studies. The reactivity of spin−orbit excited Cl($^2P_{1/2}$) atoms toward ethane was examined. The rate constant for reaction of Cl($^2P_{1/2}$) atoms with C_2H_6 is less than half of that for Cl($^2P_{3/2}$) atoms. The majority ($>$86%) of collisions between Cl($^2P_{1/2}$) and C_2H_6 lead to relaxation to Cl($^2P_{3/2}$). The motivation of the present study was to address the question "To what extent does the small (0.71% at 298 K) population of Cl($^2P_{1/2}$) contribute to the observed overall reactivity of Cl atoms toward organic compounds?" We show herein that under ambient conditions spin−orbit excited Cl($^2P_{1/2}$) atoms are responsible for $<$0.4% and $<$1.4% of the observed reactivity of thermalized Cl atoms toward C_2H_6 and C_2D_6. As discussed above, the reactivity of spin−orbit ground-state Cl($^2P_{3/2}$) atoms toward CH_3F and CH_3CH_2F measured in the present work is indistinguishable from that reported in previous studies of the kinetics of thermalized, 0.71% Cl($^2P_{1/2}$) + 99.29% Cl($^2P_{3/2}$), Cl atoms. It can be concluded that spin−orbit excited Cl($^2P_{1/2}$) atoms do not make a major contribution to the reactivity of thermalized Cl atoms toward CH_3F and CH_3CH_2F. From the admittedly limited data available, it appears that the small (0.71% at 298 K) population of Cl($^2P_{1/2}$) does not make a significant contribution to the observed overall reactivity of Cl atoms toward organic compounds.

Acknowledgment. We thank the Japanese government for a NEDO grant which made this collaborative research possible, and Masahiro Kawasaki (Kyoto University), Gus Hancock (Oxford University) and Ciara Breheny (Oxford University) for helpful discussions. This work was also partly supported by Grants-in-Aid from the Ministry of Education, Science, and Culture of Japan.

References and Notes

(1) *Atmospheric Chemistry and Global Change*; Brasseur, G. P., Orlando, J. J., Tyndall, G. S., Eds.; Oxford Univ Press: Oxford, U.K., 1999.
(2) Finlayson-Pitts, B. J.; Pitts, J. N. *Chemistry of the Upper and Lower Atmosphere: Theory, Experiments and Applications*; Academic Press: San Diego, CA, 2000.
(3) Niki, H.; Maker, P. D.; Savage, C. M.; Breitenbach, L. P. *Int. J. Chem. Kinet.* **1980**, *12*, 1001.
(4) Orlando, J. J.; Tyndall, G. S.; Wallington, T. J. *J. Phys. Chem.* **1996**, *100*, 7026.
(5) Ninomiya, Y.; Kawasaki, M.; Guschin, A.; Molina, L. T.; Molina, M. J.; Wallington, T. J. *Environ. Sci. Technol.* **2000**, *34*, 2973.
(6) National Institute of Standards and Technology Chemical Kinetics Database 17, NIST, Gaithersburg, MD, 1998.
(7) Dagdigian, P. J.; Campbell, M. L. *Chem. Rev.* **1987**, *87*, 1.
(8) Matsumi, Y.; Izumi, K.; Skorokhodov, V.; Kawasaki, M.; Tanaka, N. *J. Phys. Chem. A* **1997**, *101*, 1216.
(9) Zhang, J.; Dulligan, M.; Wittig, C. *J. Chem. Phys.* **1997**, *107*, 1403.
(10) Hilbig, R.; Wallenstein, R. *IEEE J. Quantum Electron.* **1983**, *QE-19*, 1759.
(11) Zare, R. N. *Angular Momentum*; Wiley-Interscience, New York, 1988.
(12) Chichinin, A. I. *J. Chem. Phys.* **2000**, *112*, 3772.
(13) Tyndall, G. S.; Orlando, J. J.; Kegley-Owen, C. S. *J. Chem. Soc., Faraday Trans.* **1995**, *91*, 3055.
(14) Tiemann, E.; Kanamori, H.; Hirota, E. *J. Chem. Phys.* **1988**, *88*, 2457.
(15) Chichinin, A. I. *Chem. Phys. Rep.* **1996**, *15*, 843.
(16) Donovan, R. J.; Husain, D.; Bass, A. M.; Brown, W.; Davis, D. D. *J. Phys. Chem.* **1969**, *50*, 4115.
(17) Chichinin, A. I.; Krasnoperov, L. N. *Chem. Phys. Lett.* **1986**, *124*, 8.
(18) Sotnichenko, S. A.; Bokun, V. Ch.; Nadkhin, A. I. *Chem. Phys. Lett.* **1988**, *153*, 560.
(19) Chasovnikov, S. A.; Chichinin, A. I.; Kransnoperov, L. N. *Chem. Phys.* **1987**, *116*, 91.
(20) Lee, S.-H.; Liu, K. *J. Chem. Phys.* **1999**, *111*, 6253.
(21) Tyndall, G. S.; Orlando, J. J.; Wallington, T. J.; Dill, M.; Kaiser, E. W. *Int. J. Chem. Kinet.* **1997**, *29*, 43.
(22) DeMore, W. B.; Sander, S. P.; Golden, D. M.; Hampson, R. F.; Kurylo, M. J.; Howard, C. J.; Ravishankara, A. R.; Kolb, C. E.; Molina, M. J. Chemical Kinetics and Photochemical Data for use in Stratospheric Modeling. NASA JPL Publication 97-4, 1997.
(23) Atkinson, R.; Baulch, D. L.; Cox, R. A.; Hampson, R. F., Jr.; Kerr, J. A.; Rossi, M. J.; Troe, J. *J. Phys. Chem. Ref. Data* **1999**, *28*, 191.
(24) Kandel, S. A.; Rakitzis, T. P.; Lev-On, T.; Zare, R. N. *J. Chem. Phys.* **1996**, *105*, 7550.
(25) Kandel, S. A.; Rakitzis, T. P.; Lev-On, T.; Zare, R. N. *J. Phys. Chem.* **1998**, *102*, 2270.
(26) Parmar, S. S.; Benson, S. W. *J. Am. Chem. Soc.* **1989**, *111*, 57.
(27) Dobis, O.; Benson, S. W.; Mitchell, T. J. *J. Phys. Chem.* **1994**, *98*, 12284.
(28) Manning, R. G.; Kurylo, M. J. *J. Phys. Chem.* **1977**, *81*, 291.
(29) Tschuikow-Roux, E.; Niedzielski, J.; Faraji, F. *Can. J. Chem.* **1985**, *63*, 1093.
(30) Wallington, T. J.; Hurley, M. D. *Chem. Phys. Lett.* **1992**, *194*, 309.
(31) Tschuikow-Roux, E.; Yano, T.; Niedzielski, J. *J. Chem. Phys.* **1985**, *82*, 65.
(32) Tuazon, E. C.; Atkinson, R.; Corchnoy, S. B. *Int. J. Chem. Kinet.* **1992**, *24*, 639.
(33) Wallington, T. J.; Ball, J. C.; Nielsen, O. J.; Bartkiewicz, E. *J. Phys. Chem.* **1992**, *96*, 1241.